Articles

Mapping Conformational Changes in a Protein: Application of a Protein Footprinting Technique to cAMP-Induced Conformational Changes in cAMP Receptor Protein†

Noel Baichoo and Tomasz Heyduk*

Edward A. Doisy Department of Biochemistry and Molecular Biology, St. Louis University School of Medicine, 1402 South Grand Boulevard, St. Louis, Missouri 63104

Received March 27, 1997; Revised Manuscript Received June 25, 1997⊗

ABSTRACT: We have used protein footprinting [Heyduk, E., & Heyduk, T. (1994) *Biochemistry 33*, 9643] to detect and map ligand-induced conformational changes in cAMP receptor protein (CRP). The binding of cAMP to CRP dramatically increases the specific DNA binding activity of the protein and, as has been previously shown, induces conformational changes in the protein. Protein footprinting experiments with the free CRP, the CRP−cAMP complex, and the CRP-cGMP complex were analyzed quantitatively. Binding of cAMP produced measurable differences in the susceptibility of CRP to the cleavage by Fe-EDTA. Almost all of these changes occurred in the C-terminal domain (DNA binding domain) of the protein. Additional changes were observed at the ends of the C α-helix, which is involved in intersubunit contacts in the CRP dimer, and in the hinge peptide, connecting N-terminal and C-terminal domains of the protein. The boundaries of the regions in the C-terminal domain, which exhibited changes in susceptibility to Fe-EDTA cleavage, almost exactly corresponded to D, E, and F α-helices which are involved directly in the recognition of DNA. The F α-helix, which provides all base-specific contacts in the CRP−DNA complex, became hypersensitive to Fe-EDTA-mediated cleavage, whereas the solvent exposure of D and E α-helices was decreased upon binding of cAMP. These results suggest that a significant part of cAMP-induced conformational change in CRP involves a movement of secondary structure elements in the C-terminal domain of the protein so that the recognition F α-helix becomes exposed to the solvent. In contrast to cAMP, binding of cGMP produced insignificant changes in susceptibility to Fe-EDTA-mediated cleavage. This is consistent with the inability of cGMP to induce functional conformational changes in CRP. The protein footprinting technique appears to be sufficiently sensitive for detection and mapping of ligand-induced conformational changes in proteins.

Recently a high-resolution protein footprinting technique has been described (Heyduk & Heyduk, 1994) and applied to mapping contact domains of proteins involved in protein−protein (Heyduk et al., 1996; Greiner et al., 1996) and protein−DNA interactions (Heyduk & Heyduk, 1994). Contact domains of the protein for interactions with other macromolecules are identified in this technique by observing protection against Fe-EDTA-mediated proteolysis when a protein−macromolecule complex is formed. Use of end-labeled protein allows identification of cleavage products by a simple electrophoretic procedure, and use of a small and nonspecific Fe-EDTA complex as a protease allows high-resolution probing of a protein surface. Quantitative tools for the analysis of protein footprinting data were developed (Heyduk et al., 1996) which permitted detection of small changes in the sensitivity of the protein to Fe-EDTA-mediated proteolysis. In principle, this protein footprinting technique should be applicable to studies of any processes which result in changes of solvent accessibility of the protein backbone. Solvent accessibility seems to be the most important parameter determining the efficiency of the Fe-EDTA-mediated cleavage of a protein molecule (Ermacora et al., 1992, 1996). In this work we used the protein footprinting technique to study conformational changes in cAMP receptor protein (CRP)[1] induced by cAMP binding.

CRP is a bacterial protein involved in regulation of a large number of genes [for a recent review, see Kolb et al. (1993)]. The protein elicits its biological functions through cAMP-regulated binding to specific sites of promoter DNA. The binding of cAMP to CRP dramatically increases the specific DNA binding activity of the protein and was shown to involve conformational changes in the protein (Krakow & Pastan, 1973; Wu & Wu, 1974; Wu et al., 1984; Eilen & Krakow, 1977; Pampeno & Krakow, 1979; Tsugita et al., 1982; Ebright et al., 1985; Heyduk & Lee, 1989; DeGrazia et al., 1990; Lee et al., 1990; Tan et al., 1992; Hinds et al., 1992; Sixl et al., 1992). The nature of these changes remains

† This work was supported by National Institutes of Health Grant GM50514.

* Corresponding author: Telephone: (314) 577-8152. Telefax: (314) 577-8156. E-mail: heydukt@wpogate.slu.edu.

⊗ Abstract published in *Advance ACS Abstracts,* August 15, 1997.

[1] Abbreviations: CRP, cAMP receptor protein; CRP#, a derivative of CRP labeled specifically at the N-terminus with ^{33}P; HMPK, heart muscle protein kinase; ANS, 8-anilino-1-naphthalenesulfonic acid; LB, Luria broth.

S0006-2960(97)00714-9 CCC: $14.00

to be determined since only the X-ray three-dimensional structure of the cAMP−CRP complex (McKay et al., 1982; Weber & Steitz, 1987) and cAMP−CRP−DNA complex (Schultz et al., 1991; Parkinson et al., 1996) are known. The three-dimensional structure of the free protein is not yet available. The cAMP-induced conformational change of CRP must involve communication between different regions of the protein since the binding of cAMP occurs in the domain of CRP which is spatially separated from the DNA binding domain (McKay et al., 1982; Weber & Steitz, 1987; Schultz et al., 1991; Parkinson et al., 1996). Quantitative analysis of the energetics of intersubunit contacts in CRP showed that both intersubunit and interdomain interactions (Cheng et al., 1993, 1995) play a significant role in a communication between cAMP and DNA binding sites. A model for cAMP-induced conformational changes in CRP has been proposed on the basis of results of mutagenesis experiments (Garges & Adhya, 1985, 1987; Kim et al., 1992; Ryu et al., 1993).

In this work, we use the example of cAMP-induced conformational change of CRP to show that our protein footprinting technique can be used to detect and map conformational changes in proteins. The regions of CRP affected by binding of cAMP were identified and mapped by detecting the changes in the sensitivity to Fe-EDTA-mediated proteolysis.

MATERIALS AND METHODS

Expression and Purification of HMPK−CRP−His$_6$. The pQE60NB1, a vector for expression of HMPK−CRP−His$_6$ (CRP derivative with cAMP-dependent protein kinase recognition site at the N-terminus and hexahistidine at the C-terminus), was constructed by cloning a PCR-generated *crp* gene from pPLcCRP plasmid (a gift from Dr. A. Gronenborn, NIDDKD) into pQE60 plasmid (Qiagen, Inc.). PCR primers used for amplification of the *crp* contained sequences encoding an N-terminal protein kinase recognition site (VRRAS) and *Nco*I and *Bgl*II restriction sites. The amplified DNA was digested with *Nco*I and *Bgl*II restriction enzymes and subcloned between *Nco*I and *Bgl*II restriction sites of pQE60. Several clones of pQE60NB1 plasmid were sequenced, and the clones with no PCR-generated errors were used for subsequent protein expression. The expressed CRP protein derivative had the following structure: MVRRAS<u>V</u>-CRP-RSHHHHHH, where the nonnative amino acids are shown in a single letter code (a serine residue which is phosphorylated by protein kinase is underlined) and CRP represents the native protein sequence. Protein was expressed in *Escherichia coli* M15 cells containing pREP4 plasmid (Qiagen, Inc.). The cells were shaken at 37 °C in 1 L of LB (Miller, 1972) containing 100 μg/mL ampicillin and 25 μg/mL kanamycin until $OD_{600} = 0.7-0.9$. Recombinant protein expression was induced by addition of isopropyl β-D-thiogalactoside to 0.2 mM, and the cells were shaken for an additional 5 h at 37 °C. The cells were harvested by centrifugation (10000*g*; 10 min at 4 °C) and stored frozen at −70 °C until used. The HMPK−CRP−His$_6$ protein was purified as described previously for the native CRP (Heyduk & Lee, 1989).

Activity of HMPK−CRP−His$_6$. The cAMP binding activity and the specific DNA binding activity of the HMPK−CRP−His$_6$ derivative were tested to determine if the addition of nonnative sequences affected the structure of CRP.

The cAMP binding was measured by a fluorescence titration of the protein−(8-anilino-1-naphtalenesulfonic acid (ANS) complex as described previously for wild-type CRP (Heyduk & Lee, 1989). ANS binds to CRP with a low affinity and with a dramatic increase of fluorescence, and cAMP quenches fluorescence of CRP-bound ANS (Heyduk & Lee, 1989). Therefore, the binding of cAMP can be conveniently followed using the fluorescence signal of CRP-bound ANS. A solution of 2.9 μM CRP in 600 μL of 50 mM Tris (pH 7.8), 100 mM KCl, and 1 mM EDTA containing 25 mM ANS was titrated with small aliquots of concentrated cAMP. Fluorescence of ANS (excitation at 350 nm and emission at 480 nm) was recorded after each addition of cAMP. The results of the titration were plotted as a relative change of fluorescence ($\Delta F/F_0$) vs cAMP concentration and were fitted to an equation describing binding of cAMP to CRP (Heyduk & Lee, 1989) using a nonlinear regression.

The DNA binding activity of the CRP derivative was determined by measuring binding, with and without cAMP, of HMPK−CRP−His$_6$ to a 26 bp DNA fragment containing the wt *lac* CRP binding site (5′-ATTAATGTGAGTTAGCT-CACTCATTA-3′). The DNA fragment was labeled at the 5′ end with a fluorochrome (CPM, *N*-[4-[7-(diethylamino)-4-methylcoumarin-3-yl]phenyl]maleimide) (Heyduk & Lee, 1990). Formation of the HMPK−CRP−His$_6$−DNA complex was followed by a change of fluorescence polarization of the fluorochrome-labeled DNA fragment (Heyduk & Lee, 1990). A solution of the 9.8 nM fluorochrome-labeled 26 bp DNA fragment in 600 μL of 50 mM Tris (pH 7.8), 150 mM KCl, 1 mM EDTA, and 200 μM cAMP (when present) was titrated with small aliquots of concentrated HMPK−CRP−His$_6$. After each addition, the fluorescence anisotropy of fluorochrome-labeled DNA was measured (excitation at 390 nm, emission at 480 nm). Fractional saturation of DNA with the protein was calculated by dividing the anisotropy change at a given protein concentration by a maximal anisotropy change (measured at a large excess of the protein). The equilibrium association constant for protein−DNA complex formation was determined by a nonlinear regression analysis of fluorescence titration data as described previously (Heyduk & Lee, 1990). In all of the above measurements the concentration of the protein was calculated assuming that the preparation of HMPK−CRP−His$_6$ was 100% active, as previously assumed in the case of wild-type protein (Heyduk & Lee, 1990).

Phosphorylation of the HMPK−CRP−His$_6$ Derivative. The HMPK−CRP−His$_6$ derivative was labeled with ^{33}P in a reaction mixture (300 μL) containing 17 μM CRP, 188 units of bovine heart muscle cAMP-dependent protein kinase (catalytic subunit; Sigma, P2645), 0.2 μM [γ^{33}P]ATP (70 TBq/mmol; NEN), 20 mM Tris-HCl (pH 7.5), 1 mM DTT, 100 mM NaCl, and 12 mM $MgCl_2$. The reaction was carried out for 1 h at 37 °C, after which 20 μL of Ni^{2+}−NTA−agarose (Qiagen) suspension was added to the labeling reaction. After incubation for 15 min at room temperature (with gentle shaking), the Ni^{2+}−NTA−agarose was washed twice with 20 mM Tris-HCl (pH 7.5), 1 mM DTT, and 100 mM NaCl (200 μL). After each wash the sample was centrifuged (1 min at 1000*g*, 4 °C), and the supernatant was discarded. The ^{33}P-labeled CRP derivative (CRP$^{\#}$) was eluted by suspending the Ni^{2+}−NTA−agarose in 20 mM Tris-HCl (pH 7.5), 1 mM DTT, 100 mM NaCl, and 0.5 M

imidazole. The suspension was gently shaken at room temperature for 15 min. Ni^{2+}−NTA−agarose was precipitated by centrifugation for 1 min at 1000*g*, and the supernatant was collected. The CRP# was dialyzed overnight against 10 mM MOPS−NaOH (pH 7.2), 250 mM NaCl, and 10 mM $MgCl_2$ and stored at 4 °C. Control experiments showed no incorporation of ^{33}P into the native CRP (lacking the kinase recognition site) under the above phosphorylation conditions.

Fe-EDTA Footprinting Reactions. Reaction mixtures (10 μL) contained 8.5−10 μM CRP#, 2 mM EDTA, 1 mM $(NH_4)_2Fe^{II}(SO_4)_2$, 1 mM H_2O_2, 20 mM sodium ascorbate, 10 mM MOPS (pH 7.2), 250 mM NaCl, and 10 mM $MgCl_2$. When present, cAMP and cGMP were at 400 μM. Reactions were started by simultaneous addition of EDTA and $(NH_4)_2Fe^{II}(SO_4)_2$ [as a freshly prepared 20 mM EDTA−10 mM $(NH_4)_2Fe^{II}(SO_4)_2$ mixture], H_2O_2, and sodium ascorbate. Reactions were terminated after 40 min by the addition of 5 μL of 3× sample buffer [150 mM Tris-HCl (pH 7.9), 36% glycerol, 12% SDS, 6% β-mercaptoethanol, and 0.01% bromophenol blue]. Cleavage products were separated on 16 cm × 40 cm × 0.75 mm or 16 cm × 14 cm × 0.75 mm Tricine−SDS−polyacrylamide gels (Schagger & von Jagow, 1987; Heyduk & Heyduk, 1994). Gels were dried, and their digital images were obtained with a Molecular Dynamics Model 425B Phosphorimager.

Molecular Weight Markers and Assignment of Fe-EDTA Cleavage Sites. A series of CRP# fragments, cleaved at specific residues, were generated for the purpose of assigning the Fe-EDTA cleavage sites. The fragments terminating at residues 189, 163, 157, 120, 114, and 59 were obtained by CNBr cleavage at methionines (Gross, 1967), and fragments terminating at residues 178, 92, and 18 were obtained by Cys-specific cleavages with 2-nitro-5-thiocyanatobenzoic acid (Jacobson et al., 1973). Additionally, the fragments terminating at residues 164, 140, and 120 were obtained by expressing truncated CRP templates prepared by PCR.

Reactions for methionine-specific cleavage contained (25 μL; pH 2 with 1 M HCl) 4.25 μM CRP#, 400 mM CNBr, and 0.3% SDS. After 40 min at 25 °C, reactions were terminated by freezing (15 min at −80 °C) followed by lyophilization and addition of 25 μL of 3× SDS−PAGE loading buffer. The reaction for cysteine-specific cleavage contained (115 μL) 5 μM CRP#, 0.1 M Tris (pH 8.0), 12.5 mM glycine, and 0.4 mM 2-nitro-5-thiocyanatobenzoic acid. The mixture was incubated at 37 °C for 1 h after which an equal volume of cold 10% trichloroacetic acid was added. Precipitated protein was collected by centrifugation for 10 min at 12000*g*. The pellet was washed with 200 μL of acetone, dried in a SpeedVac (Savant), and dissolved in 100 μL of 0.2 M Tris (pH 9.0) containing 9 M urea and 25 mM glycine. After 6−12 h of incubation at 37 °C an equal volume of 3× SDS−PAGE loading buffer was added, and cleaved CRP# samples were stored at −80 °C until used.

The assignment of Fe-EDTA cleavage sites was accomplished by running on the same gel Fe-EDTA-cleaved CRP# and defined CRP# fragments described above. The assignment was done by interpolation between measured mobilities of defined CRP# fragments (Heyduk et al., 1996).

Data Analysis. The data were analyzed as described previously (Heyduk et al., 1996). Briefly, phosphorimager intensities were integrated across full lane widths and plotted versus electrophoretic mobility using ImageQuant (Molecular Dynamics). Phosphorimager intensity plots were aligned to correct for distortions between lanes using ALIGN [available on request; written in BASIC and running under LabWindows (National Instruments)]. After alignment, intensity plots were imported into SigmaPlot (Jandel Scientific), where normalization of gel-loading efficiencies, transformation of electrophoretic mobility into the position of the cleavage site in the primary structure of CRP, and preparation of difference plots were performed using routines written in SigmaPlot transform language (available on request). The final product of this analysis is a difference plot (examples: Figures 2 and 3) which shows $(I - I_{CRP^\#})/I$ vs residue number, where I is the corrected Phosphorimager intensity for the complex under study and $I_{CRP^\#}$ is the corrected Phosphorimager intensity for CRP# alone.

RESULTS

Activity of HMPK−CRP−His$_6$. We have used in our experiments CRP protein which was modified by the addition of seven nonnative amino acid residues to the N-terminus and eight nonnative amino acid residues to the C-terminus of the protein. Therefore, the control experiments were conducted to determine if this modification affected the functions of CRP. Since the goal of this work was to investigate the cAMP-induced conformational changes of CRP, the ability of the HMPK−CRP−His_6 derivative to bind cAMP and undergo the functional conformational changes was tested.

Figure 1A shows the results of the cAMP binding experiment using fluorescence titration of the protein−ANS complex (Heyduk & Lee, 1989). The HMPK−CRP−His_6 protein was able to bind cAMP with an affinity essentially identical to the one observed for the wt CRP [the association equilibrium constant was 1.9×10^4 M^{-1} in the case of HMPK−CRP−His_6 compared to 2.3×10^4 M^{-1} in the case of wt CRP (Heyduk & Lee, 1989)].

Figure 1B shows the results of a DNA binding experiment. The HMPK−CRP−His_6 protein was able to bind to a DNA fragment containing a CRP binding site from the *lac* operon in a cAMP-dependent fashion. The equilibrium association constant for the HMPK−CRP−His_6 protein was 7.9×10^7 M^{-1}, which was comparable to the binding constant of 2.0×10^7 M^{-1} measured for the wt CRP under the same experimental conditions (Heyduk & Lee, 1992). Since the appearance of specific DNA binding activity in CRP upon cAMP binding requires that a functional conformational change in the protein occur, we concluded that the HMPK−CRP−His_6 derivative underwent the same conformational changes in response to cAMP binding as the wild-type protein.

Additionally, HMPK−CRP−His_6 was able to interact with RNA polymerase in solution in the absence of promoter DNA (not shown) as observed for the wt protein (Heyduk et al., 1993). The HMPK−CRP−His_6 protein was also able to stimulate *in vitro* transcription using CRP-dependent promoter fragments as templates (not shown). These data indicate that the addition of amino acid sequences to the N- and the C-terminus of CRP did not significantly change any of the functional properties of the protein and that the results obtained with the HMPK−CRP−His_6 protein are valid for the wt CRP.

Protein Footprinting of the CRP−cAMP Complex. Figure 2A (upper panel) shows as an example a gel image for a

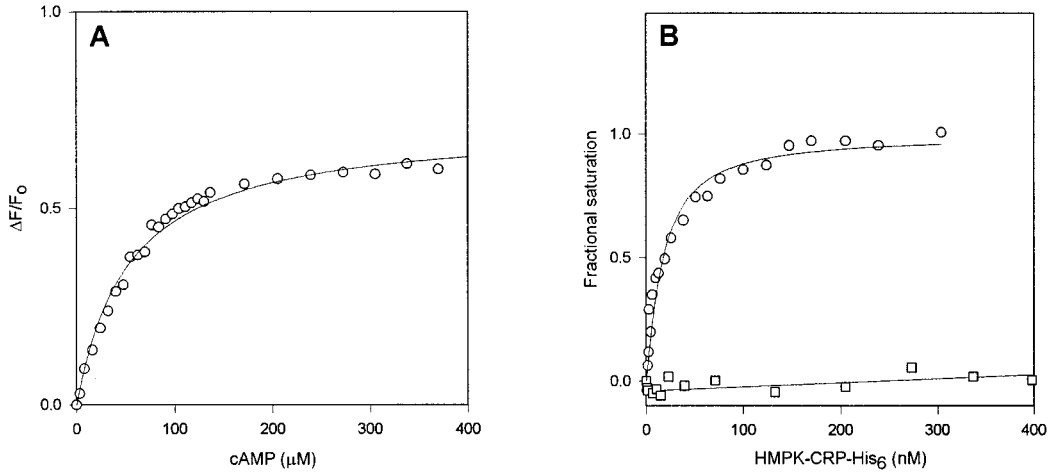

FIGURE 1: Activity of HMPK−CRP−His_6. (A) The cAMP binding isotherm. The relative fluorescence change of the protein−ANS complex is plotted as a function of cAMP concentration. The solid line represents the best fit to the equation describing the binding of cAMP to the first binding site of CRP as described by Heyduk and Lee (1989). The fitted equilibrium binding constant was 1.9×10^4 M^{-1}. (B) The DNA binding isotherm in the presence of 200 μM cAMP (open circles) and in the absence of cAMP (open squares). The solid line represents the best fit to an equation describing the formation of the 1:1 CRP−DNA complex (Heyduk & Lee, 1990). The fitted equilibrium association constant was 7.9×10^7 M^{-1}. The binding was monitored by measuring a change in fluorescence anisotropy of the 26 bp fluorochrome-labeled DNA fragment containing the *lac* CRP binding site (Heyduk & Lee, 1990). Fractional saturation was calculated as a ratio of the observed change in anisotropy to the maximal change of anisotropy observed at saturation.

protein footprinting experiment with CRP$^{\#}$ alone and with the CRP$^{\#}$−cAMP complex. Cleavage reactions in footprinting experiments have to be performed under "single hit" conditions (Brenowitz et al., 1988). Thus, typically in our experiments no less than 90% of the protein remained uncut (Figure 2). Visual comparison of gel lanes for CRP$^{\#}$ footprinting experiments in the absence and in the presence of cAMP revealed differences in intensities of some bands, mostly in the region of the gel corresponding to the C-terminal domain of CRP (Figure 2A). Since these changes were rather small, it appears that relying on just the visual comparison of band intensities between the lanes is not sufficient. Therefore, the data were subjected to a quantitative, objective data analysis (Heyduk et al., 1996). The quantitative analysis involved correction for gel-loading and cleavage efficiency differences between the lanes and the transformation of the electrophoretic mobility of the bands into residue numbers. The final result of this quantitative analysis is a difference plot (Figure 2A, lower panel) in which the normalized differences between band intensities at corresponding positions of the lanes are plotted as a function of residue number. In this method of data presentation, a value of 0 on the *y*-axis corresponds to no difference in the intensity between corresponding bands, negative values represent protection, and positive values represent hypersensitivity. Application of the quantitative analysis revealed a clear pattern of changes in susceptibility to Fe-EDTA-mediated cleavage in the presence of cAMP. There were regions of CRP where cAMP binding resulted in protection against the cleavage, and there were regions where an increase in susceptibility to cleavage was observed (Figure 2A, lower panel).

In the presence of cGMP, in contrast to the cAMP, no differences in band intensities were apparent by visual inspection, and no significant differences in band intensities were detected by quantitative analysis (Figure 2B). The characteristic pattern of enhancements and protections detected in the case of cAMP was not observed. As previously shown, cGMP binds to CRP with an affinity similar to that of cAMP but fails to induce a functional conformational change in the protein (Takahashi et al., 1980; Fried & Crothers, 1984).

In order to show that the differences in susceptibility to Fe-EDTA-mediated cleavage detected in the presence of cAMP (Figure 2A) are real and reproducible, multiple independent repeats of footprinting experiments (such as those illustrated in Figure 2) were performed. The results of these experiments were subjected to quantitative analysis, as described above, and the resulting difference plots from the individual experiments were averaged. Figure 3A shows the averaged difference plot illustrating the effect of cAMP binding on susceptibility of CRP to Fe-EDTA-mediated cleavage. Comparison of Figure 2A (bottom panel) and Figure 3A shows that after extensive averaging of the results from multiple independent experiments the cAMP-induced enhacements and protections remained unchanged. Also, since multiple sets of independent experiments were averaged, it was possible to estimate the error of the data (error bar shown to the left of the plot). It is apparent that there are numerous deviations from the 0 value in a difference plot shown in Figure 3A which are larger than the error of the data. Thus, we concluded that the changes in susceptibility to Fe-EDTA cleavage induced by cAMP binding were real and reproducible.

Using the estimated error of the data as a guide, it was possible to identify regions of CRP which underwent a significant change in susceptibility to Fe-EDTA-mediated proteolysis upon binding of cAMP. Regions 105−117, 129−140, and 181−192 showed increased susceptibility to Fe-EDTA-mediated cleavage, and regions 140−155 and 162−180 showed decreased susceptibility to Fe-EDTA mediated cleavage. Significant changes are defined as those for which the differences between a difference plot for a given complex and the baseline (Figure 3A) were bigger than 2× standard error. All significant changes induced by cAMP were observed in the C-terminal domain (DNA binding domain of CRP) and in a long C α-helix (including a hinge region connecting α-helices C and D) which is involved in intersubunit contacts in the CRP dimer (McKay et al., 1982; Weber & Steitz, 1987). Interestingly, no significant changes

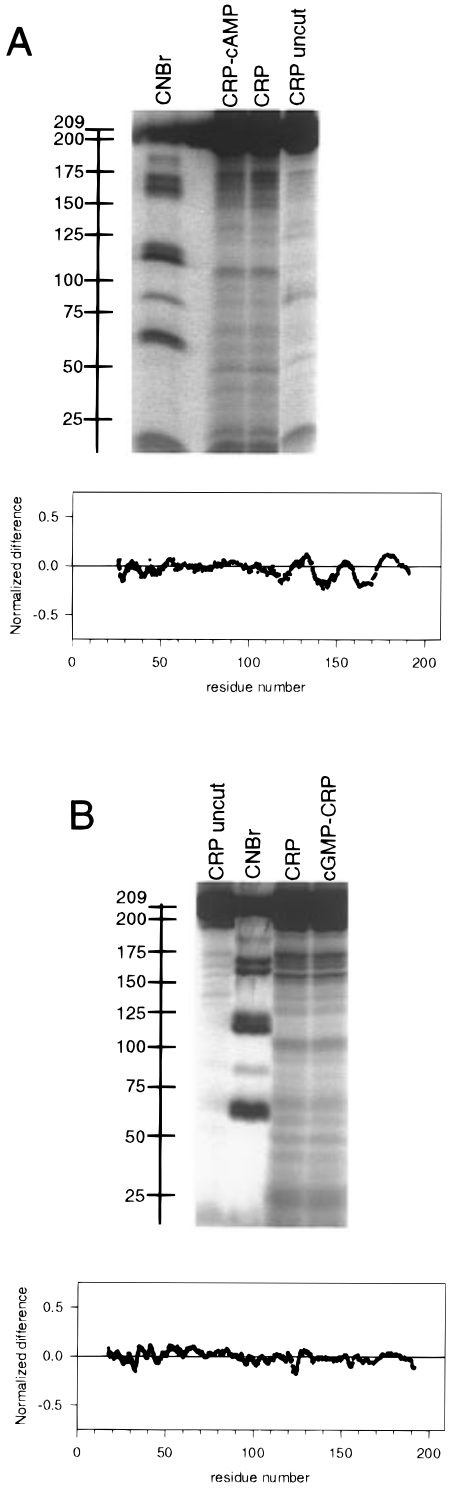

FIGURE 2: Autoradiogram of a protein footprinting SDS−PAGE for CRP# and its complexes with cAMP (A, upper panel) and cGMP (B, upper panel). Lower panels show difference plots, a result of quantitative analysis of the data shown in the upper panels. Difference plots show the normalized difference in Phosphorimager intensities versus residue number. The normalized difference is defined as $(I - I_{CRP^{\#}})/I$, where I is the corrected Phosphorimager intensity for the complex under study and $I_{CRP^{\#}}$ is the corrected Phosphoimager intensity for CRP# alone. The lanes labeled CRP uncut were loaded with samples of CRP# which was not exposed to Fe-EDTA cleavage. The lanes labeled CNBr were loaded with a sample of CRP# which was subjected to a limited cleavage with CNBr as described in Materials and Methods. All other lanes were loaded with samples of free CRP# and CRP# complexes (as indicated by the labels) subjected to Fe-EDTA-mediated cleavage. The numbers to the left of upper panels show the assigned mobility of cleavage products (expressed in residue numbers of the wt CRP).

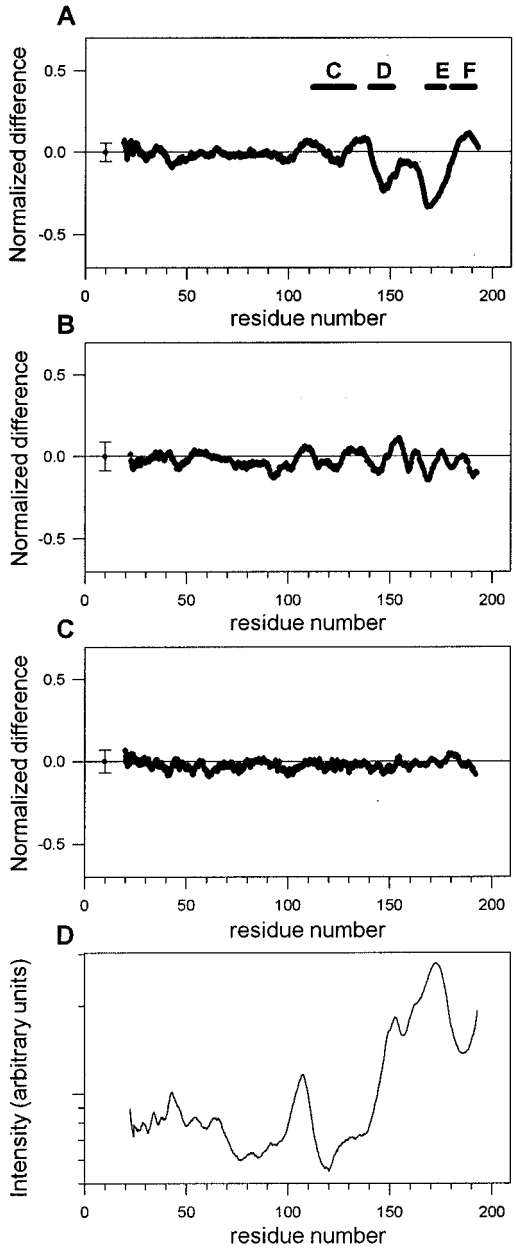

FIGURE 3: Summary of the quantitative analysis of protein footprinting data for cAMP−CRP# and cGMP−CRP# complexes. Multiple independent experiments such as those shown in Figure 2 (upper panels) were performed, the data were subjected to quantitative analysis, and the resulting difference plots (examples: Figure 2, lower panels) were averaged. (A) Averaged difference plot for the cAMP−CRP# complex vs CRP#. Boundaries of α-helices C, D, E, and F of CRP are shown schematically by thick lines and corresponding capital letters. (B) Averaged difference plot for the cGMP−CRP# complex vs CRP# alone. (C) Averaged difference plot for CRP# vs CRP# (D) Plot of the corrected Phosphorimager intensities for CRP#. Error bars shown represent a typical error (2 × standard error) of averaged plots.

were observed in the N-terminal domain of the protein, where cAMP binding occurs.

Figure 3B shows the averaged difference plot illustrating the effect of cGMP binding on the susceptibility of CRP to Fe-EDTA-mediated proteolysis. In agreement with the result shown in Figure 2B (bottom panel), the averaged difference plot in this case did not show any significant effect of cGMP.

Additionally, control data analysis was performed to determine if the quantitative data analysis and data averaging employed in Figure 3A,B did not introduce some nonrandom

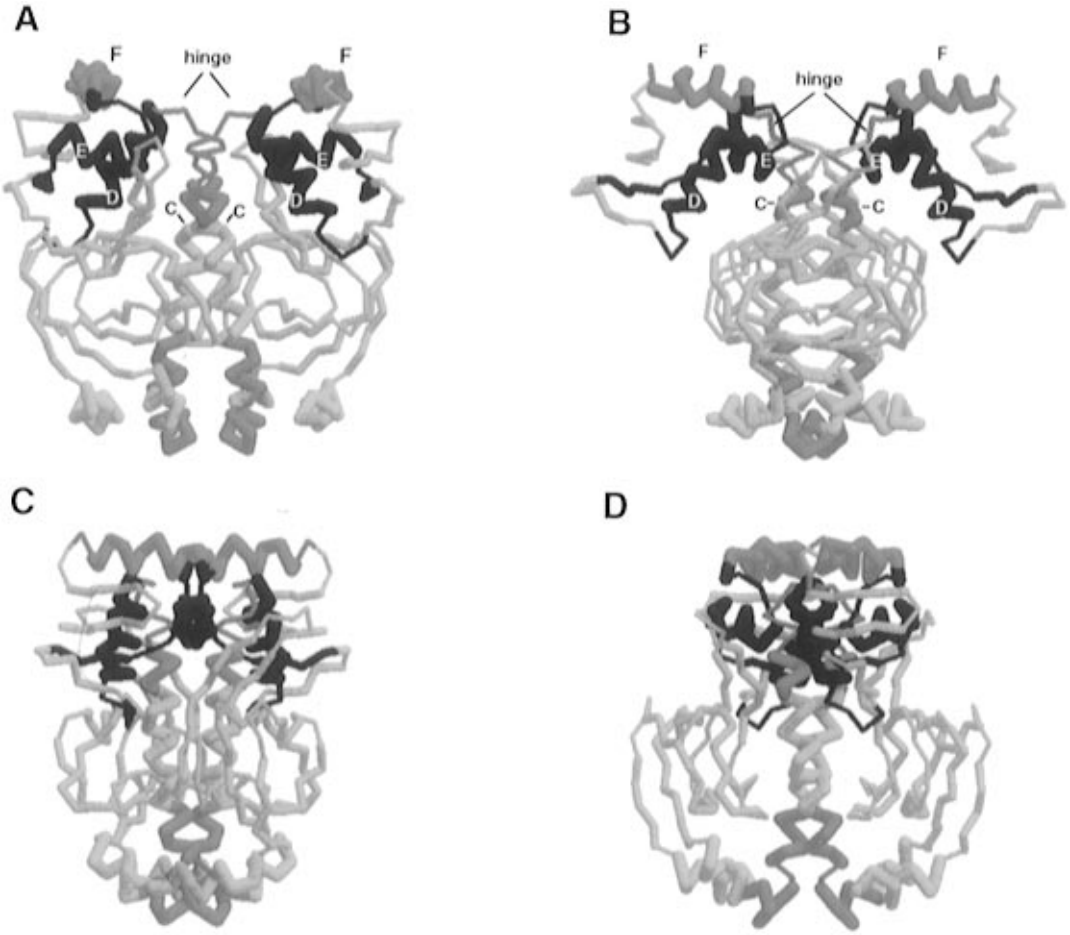

FIGURE 4: Localization of protein regions affected by cAMP binding in the three-dimensional structure of CRP. The regions of CRP which become more susceptible to the cleavage in the presence of cAMP are colored red, and the regions less susceptible to the cleavage in the presence of cAMP are colored blue. The figure was drawn with RASWIN (R. Sayle, Bio-Molecular Structure Group, Glaxo Research and Development, Greenford, U.K.) using cAMP−CRP coordinates for cAMP−CRP−DNA complex (Schultz et al., 1991). The coordinates were obtained from Brookhaven Protein Data Bank (accession code 1CGP). Panels A−D show different views of the protein approximately perpendicular to the long axis of C α-helix and differ by a relative rotation of the protein by 45°. The α-helices are shown as thick lines. In panels A and B, positions of C, D, E, and F α-helices and the position of the hinge region are indicated by corresponding labels.

trends into the data. Figure 3C shows the averaged difference plot in which band intensities for free CRP for different experiments are compared. As expected in this case, all *y*-values were clustered around zero.

Figure 3D shows the plot of averaged intensity of the bands plotted as a function of the residue number. As observed previously (Heyduk & Heyduk, 1994), the C-terminal domain of CRP seems to be more susceptible to cleavage with Fe-EDTA compared to the N-terminal domain.

It should be emphasized that, in comparison to the protection against Fe-EDTA-mediated proteolysis induced by formation of a protein−DNA complex (Heyduk & Heyduk, 1994) or protein−protein complex (Heyduk et al., 1996), the changes produced by cAMP-induced conformational changes in CRP are smaller (∼25% change in susceptibility to Fe-EDTA-mediated proteolysis). These small changes could barely be detected by a simple visual inspection of protein footprinting gels (Figure 2A) but become obvious when quantitative data analysis and extensive data averaging are performed (Figure 3A).

DISCUSSION

There is ample evidence to suggest that the CRP protein undergoes allosteric conformational changes upon binding of cAMP (Krakow & Pastan, 1973; Wu & Wu, 1974; Wu et al., 1984; Eilen & Krakow, 1977; Pampeno & Krakow, 1979; Tsugita et al., 1982; Ebright et al., 1985; Heyduk & Lee, 1989; DeGrazia et al., 1990; Lee et al., 1990; Tan et al., 1992; Hinds et al., 1992; Sixl et al., 1992). These changes are responsible for the higher affinity and the higher specificity of DNA binding by CRP in the presence of cAMP and are a key element of the biological function of the protein. On the basis of the results of mutagenesis studies, Garges and Adhya (1985, 1987) suggested a model for this conformational change in which cAMP binding induced a rearrangement of a hinge region connecting the N- and C-terminal domains of CRP. They proposed that this rearrangement would result in pushing the F α-helix of CRP away from the body of the protein so that the solvent-exposed residues of the helix protrude out of the protein bulk, thus enabling specific contacts of the F α-helix with the residues in the major groove of DNA. The F α-helix of CRP provides all base-specific contacts in the CRP−DNA complex (Schultz et al., 1991; Parkinson et al., 1996). Extensive mutagenesis data supported this model (Kim et al., 1992; Ryu et al., 1993). However, the experiments directly testing the proposed model are still lacking. Moreover, Cheng and Lee (1994) showed that relying solely on mutagenesis data without biophysical characterization of mutant proteins may result in erroneous interpretations.

Figure 4 shows the localization of CRP regions affected by cAMP binding, detected by protein footprinting experiments. In agreement with the biological effect of cAMP (increased affinity and specificity of DNA binding) the majority of the changes were detected in the C-terminal domain of CRP, where the DNA binding occurs. The boundaries of the regions in the C-terminal domain which exhibited changes in susceptibility to Fe-EDTA cleavage almost exactly corresponded to D, E, and F α-helices (Figure 4) which were involved directly in the recognition of DNA (Schultz et al., 1991; Parkinson et al., 1996). This suggests that cAMP-induced changes in the C-terminal domain most likely involve rearrangement (rigid body movement) of the secondary structure elements of this domain. This rearrangement results in a relative decrease of solvent exposure of α-helices D and E and in a relative increase in solvent exposure of the recognition F α-helix. Also, the hinge region (Figure 4) between α-helices C and D was affected (increased exposure to a solvent) by cAMP binding. These results are therefore consistent with the model of cAMP-induced conformational change (Garges & Adhya, 1985, 1987; Kim et al., 1992; Ryu et al., 1993) in which the reorientation of the hinge region resulting in pushing away of the F α-helix from the body of the protein and its proper exposure to the solvent is involved in conferring the increased DNA affinity to the CRP protein upon cAMP binding.

Our protein footprinting experiments additionally revealed that the N- and C-terminal ends of the C α-helix (Figure 4) which is involved in intersubunit contacts in the CRP dimer (McKay et al., 1982; Weber & Steitz, 1987) become more exposed to the solvent upon binding of cAMP. This is consistent with earlier observations that these regions become accessible to attack by a variety of proteolytic enzymes upon binding of cAMP (Krakow & Pastan, 1973; Ebright et al., 1985; Heyduk & Lee, 1989; Tsugita et al., 1982; Angulo & Krakow, 1985). Also, this result is consistent with the fact that intersubunit interactions are an important element in transmission of the information from the cAMP binding site in the N-terminal domain to the DNA binding site in the C-terminal domain of the protein.

In summary, the results described here provided new direct experimental data regarding the nature of allosteric conformational changes in the CRP protein. Additionally, our results showed that the protein footprinting technique is sufficiently sensitive to study ligand-induced conformational changes in proteins. The use of quantitative analysis tools (Heyduk et al., 1996) allowed objective assignments of regions where susceptibility to Fe-EDTA-mediated proteolysis changed. Protein footprinting is a unique tool which allows both the detection of conformational changes and the mapping of protein regions affected by these conformational changes.

ACKNOWLEDGMENT

We thank Drs. Joel Eissenberg, Claudette Klein, Ewa Heyduk, and Sandhya Callaci for critically reading the manuscript.

REFERENCES

Angulo, J. A., & Krakow, J. S. (1985) *Arch. Biochem. Biophys. 236*, 11−16.

Brenowitz, M., Senear, D. F., Shea, M., & Ackers, G. K. (1988) *Methods Enzymol. 130*, 132−181.

Cheng, X., & Lee, J. C. (1994) *J. Biol. Chem. 269*, 30781−30784.

Cheng, X., Gonzales, M. L., & Lee, J. C. (1993) *Biochemistry 32*, 8130−8139.

Cheng, X., Kovac, L., & Lee, J. C. (1995) *Biochemistry 34*, 10816−10826.

DeGrazia, H., Harman, J. G., Tan, G. S., & Wartell, R. M. (1990) *Biochemistry 29*, 3557−3562.

Ebright, R. H., Le Grice, S. F., Miller, J. P., & Krakow J. S. (1985) *J. Mol. Biol. 182*, 91−107.

Eilen, E., & Krakow, J. S. (1977) *J. Mol. Biol. 114*, 47−60.

Ermacora, M. R., Ledman, D. W., Hellinga, H. W., Hsu, G. W., & Fox, R. O. (1992) *Biochemistry 33*, 13625−13641.

Ermacora, M. R., Ledman, D. W., & Fox, R. O. (1996) *Nat. Struct. Biol. 3*, 59−66.

Fried, M. G., & Crothers, D. M. (1984) *J. Mol. Biol. 172*, 241−262.

Garges, S., & Adhya, S. (1985) *Cell 41*, 745−751.

Garges, S., & Adhya, S. (1987) *J. Bacteriol. 170*, 1417−1422.

Greiner, D., Hughes, K., Gunasakera, A., & Meares, C. F. (1996) *Proc. Natl. Acad. Sci. U.S.A. 93*, 71−75.

Gross, E. (1967) *Methods Enzymol. 11*, 238−255.

Heyduk, T., & Lee, J. C. (1989) *Biochemistry 28*, 6914−6924.

Heyduk, T., & Lee, J. C. (1990) *Proc. Natl. Acad. Sci. U.S.A. 87*, 1744−1748.

Heyduk, E., & Heyduk, T. (1994) *Biochemistry 33*, 9643−9650; (1995) *Biochemistry 34*, 15388 (correction).

Heyduk, T., Lee, J. C., Ebright, Y. W., Blatter, E. E., Zhou, Y., & Ebright, R. H. (1993) *Nature 364*, 548−549.

Heyduk, T., Heyduk, E., Severinov, K., Tang, H., & Ebright, R. H. (1996) *Proc. Natl. Acad. Sci. U.S.A. 93*, 10162−10166.

Hinds, M. G., King, R. W., & Feeney, J. (1992) *Biochem. J. 287*, 627−632.

Jacobson, G. R., Schaffer, M. H., Stark, G. R., & Vanaman, T. C. (1973) *J. Biol. Chem. 248*, 6583−6591.

Kim, J., Adhya, S., & Garges, S. (1992) *Proc. Natl. Acad. Sci. U.S.A. 89*, 9700−9704.

Kolb, A., Busby, S., Buc, H., Garges, S., & Adhya, S. (1993) *Annu. Rev. Biochem. 62*, 749−795.

Krakow, J. S., & Pastan, I. (1973) *Proc. Natl. Acad. Sci. U.S.A. 70*, 2529−2533.

Lee, B. J., Lee, S. J., Hayashi, F., Aiba, H., & Kyogoku, Y. (1990) *J. Biochem. 107*, 304−309.

Li, B.-J., Langer, J. A., Schwartz, B., & Pestka, S. (1989) *Proc. Natl. Acad. Sci. U.S.A. 86*, 558−562.

Miller, J. (1972) *Experiments in Molecular Genetics*, Cold Spring Harbor Laboratory, Cold Spring Harbor, NY.

McKay, D., Weber, I., & Steitz, T. (1982) *J. Biol. Chem. 257*, 9518−9524.

Pampeno, C., & Krakow, J. S. (1979) *Biochemistry 18*, 1519−1525.

Parkinson, G., Wilson, C., Gunasakera, A., Ebright, Y. W., Ebright, R. H., & Berman, H. M. (1996) *J. Mol. Biol. 260*, 395−408.

Ryu, S., Kim, J., Adhya, S., & Garges, S. (1993) *Proc. Natl. Acad. Sci. U.S.A. 90*, 75−79.

Schagger, H., & von Jaggow, G. (1987) *Anal. Biochem. 166*, 368−279.

Schultz, S., Shields, G., & Steitz, T. (1991) *Science 253*, 1001−1007.

Sixl, F., King, R. W., & Feeney, J. (1992) *Biochem. J. 266*, 545−552.

Takahashi, T., Blazy, B., & Baudras, A. (1980) *Biochemistry 19*, 5124−5130.

Tan, G.-S., Kelly, P., Kim, J., & Wartell, R. W. (1991) *Biochemistry 30*, 5076−5080.

Tsugita, A., Blazy, B., Takahashi, M., & Baudras, A. (1982) *FEBS Lett. 144*, 304−308.

Weber, I., & Steitz, T. (1987) *J. Mol. Biol. 198*, 311−326.

Wu, C.-W., & Wu, F. Y.-H. (1974) *Biochemistry 13*, 2573−2578.

Wu, F. Y.-H., Nath, K., & Wu, C.-W. (1974) *Biochemistry 13*, 2567−2572.

BI970714V